



Bright daytime light enhances circadian amplitude in a diurnal mammal

Beatriz Bano-Otalora^{a,b}, Franck Martial^b, Court Harding^b, David A. Bechtold^{a,c}, Annette E. Allen^{a,b}, Timothy M. Brown^{a,c}, Mino D. C. Belle^d, and Robert J. Lucas^{a,b,1}

^aCentre for Biological Timing, Faculty of Biology Medicine and Health, University of Manchester, Manchester M13 9PT, United Kingdom; ^bDivision of Neuroscience and Experimental Psychology, Faculty of Biology Medicine and Health, University of Manchester, Manchester M13 9PT, United Kingdom; ^cDivision of Diabetes, Endocrinology and Gastroenterology, Faculty of Biology Medicine and Health, University of Manchester, Manchester M13 9PT, United Kingdom; and ^dInstitute of Biomedical and Clinical Sciences, University of Exeter Medical School, University of Exeter, Exeter EX4 4PS, United Kingdom

Edited by Joseph S. Takahashi, The University of Texas Southwestern Medical Center, Dallas, TX, and approved April 21, 2021 (received for review January 8, 2021)

Mammalian circadian rhythms are orchestrated by a master pacemaker in the hypothalamic suprachiasmatic nuclei (SCN), which receives information about the 24 h light–dark cycle from the retina. The accepted function of this light signal is to reset circadian phase in order to ensure appropriate synchronization with the celestial day. Here, we ask whether light also impacts another key property of the circadian oscillation, its amplitude. To this end, we measured circadian rhythms in behavioral activity, body temperature, and SCN electrophysiological activity in the diurnal murid rodent *Rhabdomys pumilio* following stable entrainment to 12:12 light–dark cycles at four different daytime intensities (ranging from 18 to 1,900 lx melanopic equivalent daylight illuminance). *R. pumilio* showed strongly diurnal activity and body temperature rhythms in all conditions, but measures of rhythm robustness were positively correlated with daytime irradiance under both entrainment and subsequent free run. Whole-cell and extracellular recordings of electrophysiological activity in ex vivo SCN revealed substantial differences in electrophysiological activity between dim and bright light conditions. At lower daytime irradiance, daytime peaks in SCN spontaneous firing rate and membrane depolarization were substantially depressed, leading to an overall marked reduction in the amplitude of circadian rhythms in spontaneous activity. Our data reveal a previously unappreciated impact of daytime light intensity on SCN physiology and the amplitude of circadian rhythms and highlight the potential importance of daytime light exposure for circadian health.

circadian | light | suprachiasmatic nucleus | retina

In mammals, near-24-h (circadian) rhythms in physiology and behavior are orchestrated by a master clock located in the hypothalamic suprachiasmatic nuclei (SCN) (1, 2). The SCN clock generates a circadian rhythm in electrical activity, with neurons significantly more excited during the day (up state) than at night (down state) (3, 4). This endogenous rhythm is synchronized (entrained) to the external 24-h light–dark (LD) cycle via input from the retina (5). Thus, light exposure in the circadian night induces adjustments in circadian phase to ensure that internal time faithfully reflects external (celestial) time. Conceptual and mathematical models of light’s impact on the clock address this ability to reset circadian phase (the basis of entrainment) (6–9). However, there is evidence that another fundamental property of circadian rhythms, their amplitude, may also be influenced by light.

It is well established that the amplitude and reliability of 24-h rhythms in some aspects of physiology and behavior can be enhanced by increasing daytime light exposure (10–20). Such effects may be explained by the ability of light to directly engage some of the systems under circadian control (e.g., increasing alertness and body temperature, *T_b*) (21–23) and thus enhance rhythm amplitude de facto, without impacting the circadian clock itself. However, reports that enhanced daytime light can also lead to higher production of melatonin on the subsequent night, many hours after light exposure has ceased (12, 24–26), pose a challenge to that

explanation. The long-lasting nature of that effect raises the possibility that daytime light may have a more fundamental impact on circadian amplitude. We set out here to address this possibility by using laboratory rodents to ask whether increasing daytime irradiance produces persistent improvements in circadian amplitude and whether this can be traced back to changes in the physiological activity of the SCN circadian oscillator itself.

A challenge to studying the impact of daytime light exposure in common laboratory models (mice, hamsters, and rats) is that they are nocturnal and employ strategies to avoid light in the day (such as curling up asleep). We therefore used a diurnal rodent, *Rhabdomys pumilio* (the four-striped mouse) (27–29) which is active through the day in both the laboratory and wild, ensuring good exposure to modulations in daytime light intensity. We find that increasing irradiance across a range equivalent to that from dim indoor lighting to natural daylight enhances the reproducibility and robustness of behavioral and physiological rhythms at the whole-animal level that persist into subsequent free run in constant darkness. This effect is associated with profound differences in the electrophysiological activity of the SCN, with bright daytime light producing persistent increases in SCN excitability and enhancing

Significance

Light is an important regulator of endogenous circadian clocks. Regular light–dark cycles set circadian phase to ensure synchrony with external time, while irregular or inappropriate light exposure can disrupt circadian rhythms. We ask here whether light can also impact another key parameter of circadian rhythms, their amplitude, under conditions of stable entrainment. Using a diurnal rodent species and carefully calibrated light stimuli, we show that increasing the intensity of daytime light enhances the reproducibility and robustness of behavioral and physiological rhythms and increases the amplitude of circadian rhythms in electrical activity in the central brain pacemaker. These findings reveal an impact of light on circadian amplitude and highlight the potential importance of daytime light exposure for circadian health.

Author contributions: B.B.-O., T.M.B., M.D.C.B., and R.J.L. designed research; B.B.-O., F.M., C.H., D.A.B., A.E.A., T.M.B., and M.D.C.B. performed research and analyzed data; and B.B.-O. and R.J.L. wrote the paper with inputs from all authors.

Competing interest statement: T.M.B. and R.J.L. have received investigator-initiated grant funding from Signify (formerly Philips Lighting). R.J.L. has received honoraria from Samsung Electronics.

This article is a PNAS Direct Submission.

This open access article is distributed under Creative Commons Attribution License 4.0 (CC BY).

¹To whom correspondence may be addressed. Email: robert.lucas@manchester.ac.uk.

This article contains supporting information online at <https://www.pnas.org/lookup/suppl/doi:10.1073/pnas.2100094118/-DCSupplemental>.

Published May 24, 2021.

the amplitude of the circadian variation in spontaneous neuronal activity.

Results

Brighter Days Increase Reproducibility and Robustness of Circadian Rhythms. We first set out to determine the impact of increasing daytime light intensity on circadian rhythms in behavior (general locomotor activity and voluntary wheel-running activity) and physiology (Tb) under stable entrainment to a 12:12 LD cycle. As a previous study in this species failed to identify a pronounced impact on rhythmicity across a range of lower illuminances (29), here we applied daytime irradiances (Fig. 1A) extending into the lower portion of the natural daylight range (12.77 to 14.80 log melanopsin effective photons/cm²/s; or 18 to 1,940 lx Melanopic EDI [equivalent daylight illuminance]). Lighting conditions aimed to reproduce the *R. pumilio* experience of natural daylight by approximating the relative activation for melanopsin, rod opsin, and cone opsins (Fig. 1A; although note that we did not recreate levels of near ultraviolet [UV] required to adequately stimulate S cones for practical and safety reasons). When exposed to these lighting conditions, all animals remained entrained to the 24-h LD cycle (Fig. 1B).

R. pumilio were strongly diurnal under all light conditions, spending most of the day awake and active and being quiescent at night (Fig. 1B and C and *SI Appendix*, Fig. S1 and Table S1). Indeed, there was no significant effect of daytime irradiance on the proportion of activity occurring during the light period. Nor did daytime irradiance alter mean Tb or the total amount of general or wheel-running activity across the 24 h (*SI Appendix*, Table S1). However, at a finer timescale, activity patterns were impacted by light intensity. Thus, when we quantified the appearance of periods of sustained immobility [which in mice correspond to episodes of sleep (30)], we found these occurred less often during the day (*SI Appendix*, Table S1) and were less fragmented (lower intraday variability; Fig. 2A) under higher irradiance. Moreover, the day-to-day reproducibility of this rhythm in immobility was also positively correlated with irradiance (Fig. 2B). These findings imply that rhythmicity in this proxy for sleep is more robust under brighter days. That conclusion was supported by analysis of Tb rhythms, which also showed negative correlations between daytime irradiance and fragmentation and day-to-day variability (Fig. 2C and D).

As rhythms under entrained conditions may reflect direct effects of the LD cycle as well as the output of the circadian clock, we analyzed rhythms expressed over 4 d of constant darkness at the end of each light condition to reveal the characteristics of clock-driven rhythms in the absence of direct environmental drive. In all conditions, activity rhythms free ran from the phase adopted during the prior LD cycle, as expected for stable entrainment (Fig. 2E). Circadian formalisms predict that increasing the amplitude of an entraining stimulus can alter the phase of entrainment (7), and indeed that proved to be the case in these experiments, with rhythms becoming delayed with respect to the prior LD cycle at lower intensities (Fig. 2F). Analysis of these free-running rhythms revealed effects of daytime light intensity on further circadian properties. First, the free-running period was positively correlated with prior irradiance (Fig. 2G). Second, the percentage of variance (%V) in activity explained by the circadian rhythm (an indication of rhythm robustness) was higher in animals previously held under brighter conditions (Fig. 2H).

Impact of Daytime Irradiance on SCN Electrical Activity. The effects of prior light exposure on rhythms in subsequent constant darkness indicate a persistent effect of daytime light intensity on circadian physiology. To explore this possibility, we turned to an assessment of the central SCN circadian clock itself. To this end, we collected SCN from animals housed in either bright ($n = 4$) or dim ($n = 4$) daytime irradiances for ex vivo electrophysiological recordings.

We first recorded extracellular activity in the SCN region using multielectrode arrays (MEAs) (Fig. 3A). This method allows long-term recordings (24-h) to reveal rhythms in spontaneous firing activity. We observed rhythms in spike firing at electrode sites falling within the SCN and, on average, spontaneous firing rates (SFR) were higher during the day than at night (Fig. 3B). However, there was a dramatic difference in the activity of SCNs from dim versus bright conditions (Fig. 3C–G). First, overall spontaneous firing activity was strongly influenced by prior daytime irradiance, with mean multiunit activity (MUA) across the 24-h recording epoch significantly enhanced following the bright LD cycle (Fig. 3C, $P < 0.001$, Mann–Whitney U test). Second, rhythmicity was markedly less pronounced in the dim condition. Thus, the fraction of MEA recording sites within the SCN at which a circadian variation in MUA was detected was significantly reduced under the dim condition (bright: $n = 58/92$, ~63% versus dim: $n = 42/99$, ~42%; 4 slices per condition; $P < 0.01$ Fisher's exact test), Fig. 3D). Moreover, while there was a clear daytime peak in spontaneous activity under both conditions (Fig. 3E and F), the amplitude of that rhythm (difference in firing between peak and trough) was substantially reduced in SCN taken from animals previously held under dim conditions (Fig. 3G; $P < 0.001$, Mann–Whitney U test).

Impact of Daytime Irradiance on Single-Cell Neurophysiology in the SCN. The MEA recordings thus reveal that brighter daytime light exposure produces an SCN that is overall more active and more highly rhythmic and suggest that daytime irradiance defines important aspects of SCN electrophysiology. To explore the nature of this effect, we applied whole-cell patch recordings across the day and at night in order to determine how changes in daytime irradiance impact SCN neurophysiology at the single-cell level (Fig. 4A and B).

Across the sample of neurons recorded from both bright and dim conditions ($n = 111$ and 104, respectively, eight animals per condition), we found that the resting membrane potential (RMP) ranged from -62.5 to -21.6 mV. Across most of this range, the RMP correlated with firing rate, with more hyperpolarized neurons showing lower spontaneous activity and at the extreme being silent (Fig. 4C and D). Although depolarization generally correlated with higher firing, this was not true for the most depolarized neurons. Such cells showed depolarized low-amplitude membrane oscillations in place of spikes or, at the extreme, were depolarized silent [“hyper-excited” (31, 32) (Fig. 4C)]. Neurons in each of these neurophysiological states were recorded in both conditions; however, their distribution was different. In the bright day group, hyperpolarized silent neurons only appeared at night, with the daytime state being characterized by either firing or highly depolarized cells (Fig. 4E). By contrast, in the dim-light–exposed group, a subset of neurons was hyperpolarized silent even during the day (Fig. 4E, Day: bright versus dim, $\chi^2 = 9.322$, $P = 0.009$).

Leaving aside these categorizations, both RMP and SFR showed a strong circadian variation in the bright daytime group (Fig. 4G–J). Consistent with our multiunit data and previous reports from other species (33–37), SFR was higher during the day in these animals ($P = 0.001$, Mann–Whitney U). By contrast, rhythms in SFR and RMP were substantially dampened in the dim-day group (Fig. 4G–J) to the extent that the variation in RMP no longer reached statistical significance. Overall, SFR and RMP were higher in the bright daytime group, especially during the day phase (Fig. 4H and J, $P = 0.026$ and $P = 0.009$ for SFR and RMP, respectively, Mann–Whitney U test).

Differences in spontaneous activity and RMP between conditions could originate with disparities in intrinsic properties of the neurons and/or in the degree of extrinsic synaptic input. To evaluate these possibilities, we used voltage-clamp mode to record synaptic activity (Fig. 4F, $n = 108$ and 103 from dim and bright daytime conditions, respectively). Overall, we found higher

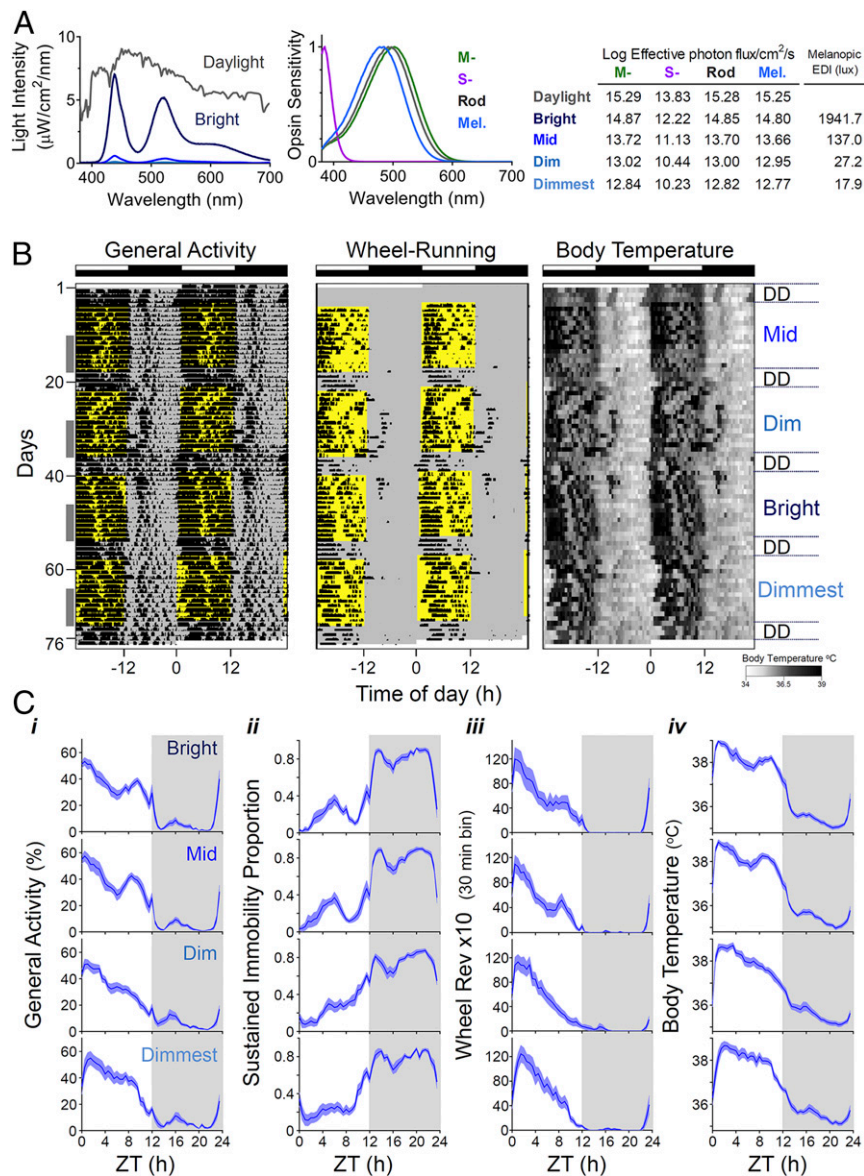


Fig. 1. Impact of increasing daytime light intensity on circadian rhythms in *R. pumilio*. (A) Lighting conditions. *Left* shows the spectral power distribution of our light source at different irradiances and that of daylight on an overcast day. *Middle* shows expected spectral sensitivity profile of mammalian rod opsin and melanopsin and *R. pumilio* medium and short wavelength-sensitive cone opsins (MWS and SWS, respectively) (61) corrected for lens transmission. *Right* table shows Log_{10} effective photon fluxes for each opsin and melanopic EDI across the different lighting stimuli used (bright, mid, dim, dimmest). (B) Double-plotted actograms for general activity, wheel running and Tb (scale below) from a representative *R. pumilio* under different lighting conditions, over a period of 2.5 mo. Time of light exposure is indicated in yellow, and intensity of the light is shown on the *Right*. Entrainment to 12:12 LD cycle at each irradiance ran for 2 wk followed by 4 d in constant darkness (DD). Note that across conditions, activity is largely restricted to daytime (light phase) coinciding with higher Tb values. However, the rhythms become less robust at low light levels. Gray columns on the left indicate the 8-d period at the end of each stage used for analysis reported in *SI Appendix, Table S1* and Fig. 2. (C) Mean waveforms for the recorded biological rhythms (*i*: general activity; *ii*: sustained immobility; *iii*: voluntary wheel-running activity; *iv*: Tb) across the different lighting conditions. Mean waveforms under bright intensities are shown in the *Top* and the dimmest conditions in panels at the *Bottom*. Values are expressed as mean \pm SEM ($n = 12$), gray areas indicate period of darkness. ZT0: ZT 0 corresponds to time of lights on.

frequency and amplitude of postsynaptic currents (PSCs) during the day than at night ($P < 0.001$, Mann–Whitney U test). However, both frequency and amplitude of synaptic inputs were similar between conditions (Fig. 4 *M* and *N*), turning the focus to alterations in intrinsic neuronal properties as a likely cause of the difference in spontaneous activity. We therefore measured input resistance (R_{input}), an intrinsic determinant of neuronal excitability. We found no differences in this parameter between experimental groups either (Fig. 4 *K* and *L*). However, we did find that R_{input} was high in *R. pumilio* SCN [as previously reported for other species (31)],

highlighting the potential for small changes in intrinsic currents to produce large modulations in RMP.

Discussion

Our experiments with *R. pumilio* reveal a fundamental and previously unappreciated effect of daytime irradiance on the SCN circadian clock. Higher daytime light intensity increased the amplitude of the SCN's daily peak in SFR and neuronal depolarization, to enhance the amplitude of its circadian rhythm in spontaneous activity. This was associated with improvements in measures of rhythm

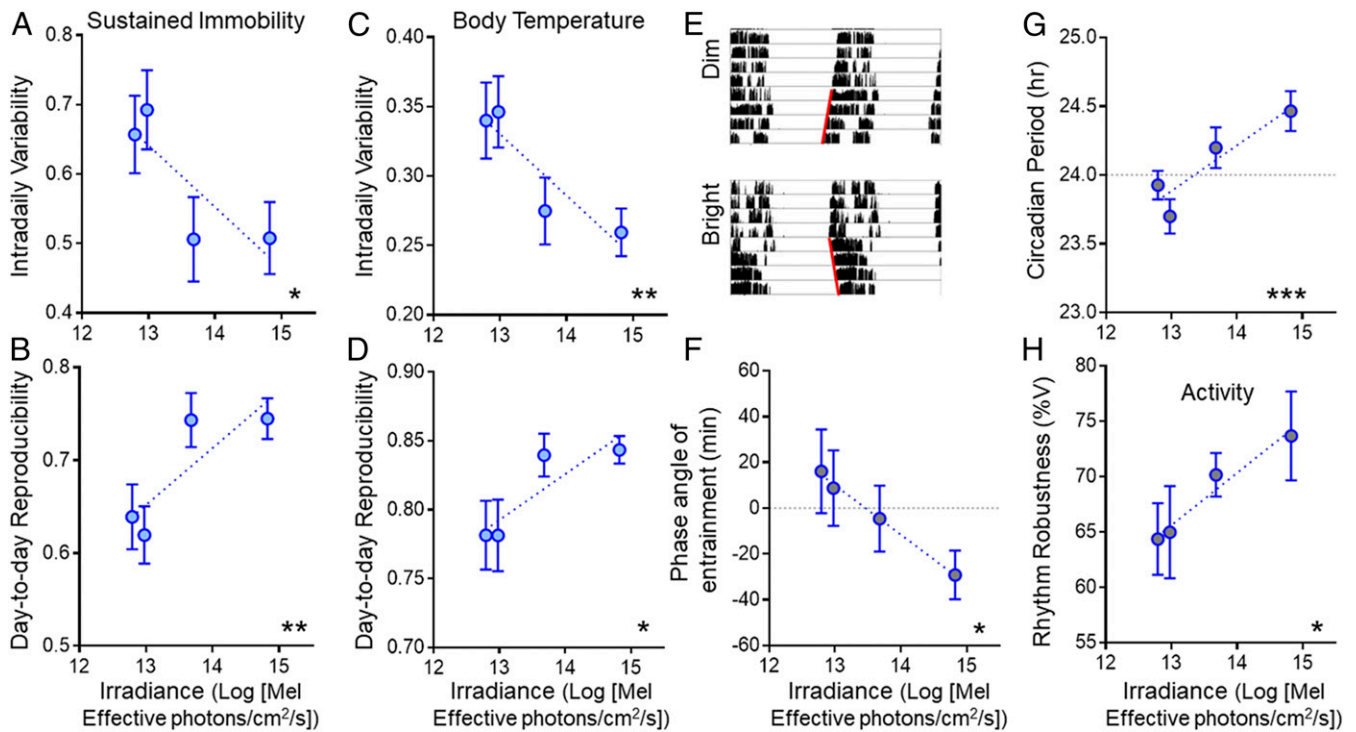


Fig. 2. Impact of increasing daytime light intensity on reproducibility and robustness of circadian rhythms under entrained and subsequent free-running conditions. (A) Intradaily variability and (B) day-to-day reproducibility of the sustained immobility rhythm as a function of daytime irradiance under entrained conditions. (C and D) Same as in A and B but for the Tb rhythm. (E) Representative wheel-running activity actogram for an *R. pumilio* over the last 4 d of entrainment under dim (Top) or bright (Bottom) irradiance, and subsequent 4 d of free run in constant darkness (note difference in slope of red lines fit to activity onsets in free run between conditions). (F) Relationship between phase angle of entrainment for wheel-running activity rhythm and daytime irradiance. (G) Free-running period and (H) robustness of the activity rhythm across all animals as a function of the prior entraining irradiance. Values are expressed as mean \pm SEM ($n = 12$, A–D; $n = 11$, F–H); significant relationships identified by linear regression (* $P < 0.05$, ** $P < 0.01$, and *** $P < 0.001$).

robustness at whole-animal level. These effects reflected a genuine long-lasting change in circadian physiology, not simply a direct and immediate response to brighter light, as they persisted once the light stimulus was removed.

The effect of daytime light intensity on rhythm amplitude and robustness reported here is not predicted by current theoretical frameworks or mathematical models of light's impact on the clock. In these formalisms, light is principally considered a modulator of circadian phase (6, 8, 9). In this capacity, light may impact amplitude transiently following disruptive changes in phase or, under very abnormal exposure patterns, by driving the oscillator toward a point of singularity (38). Neither of those effects should be engaged under the conditions of stable entrainment employed here. Under stable entrainment, the phase shifting effects of light are predicted to result in a correlation between daytime light intensity and the phase relationship between the endogenous clock and the entraining light cycle (termed the phase angle of entrainment). If the period of the entraining light cycle is substantially divergent from 24 h, phase angles of entrainment can be large [and themselves induce pathology (39)]. However, phase angles of entrainment should be less extreme when entraining and endogenous periods are fairly similar, and indeed, here we found only a modest change in phase angle (<1 h) across a wide range of daytime irradiances. The marked relationship between daytime irradiance and circadian amplitude we observe thus implies an additional impact of light exposure on the circadian machinery, distinct from its phase resetting function.

The effect of daytime light intensity reported here is also distinct from the other established way in which light can impact SCN physiology—the response to changing photoperiod. Under long photoperiods, circadian rhythms become less synchronous across

SCN neurons, resulting in a broader peak in daytime firing at the population level (40–42). We matched photoperiod across our experimental conditions, and accordingly, there was no suggestion in the MEA activity that the SCN's “up state” occupied a larger fraction of the circadian cycle in the bright condition. Moreover, our whole-cell recordings implicate a change in single-cell activity in the response to daytime light that is distinct from the changes in network behavior produced by altering photoperiod. In future work, it will be important to consider how these two effects interact. Do the longer and brighter days of summer produce even bigger changes in SCN activity than suggested by experiments changing photoperiod alone?

The most striking effect of changing entraining light intensity is on the SCN's daytime peak in spontaneous electrical activity (“up state”). Multiunit recordings reveal a dramatic reduction in daytime spiking activity under entrainment to dim daytime light. This effect is also apparent in the whole-cell recordings, in which it is revealed to originate with a shift to more hyperpolarized RMPs, and the anomalous appearance of electrically silent neurons during the day phase. Importantly, in neither MEA nor whole-cell recordings was there a corresponding increase in night-time firing in the dim light condition. Rather MEA recordings revealed a significant reduction in MUA over the subjective night (this effect did not reach significance for the whole-cell dataset likely because of the smaller number of neurons sampled). These findings are informative as they exclude desynchrony in circadian phase across the SCN neuronal population as an explanation for low rhythm amplitude—which should blunt both daytime peak and nighttime trough in activity. Rather, they point to a more fundamental reduction in SCN excitability, which disproportionately impacts the daytime peak [perhaps because more of the SCN neuronal

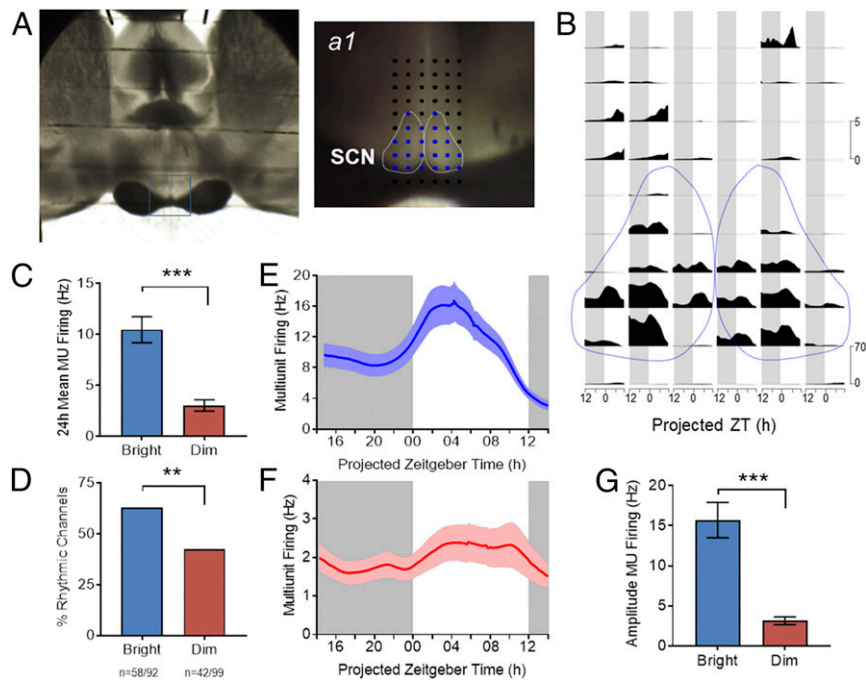


Fig. 3. Impact of daytime irradiance on SCN activity. (A) Image of a brain slice of *R. pumilio* placed over the electrode terminals of a 60-channel array to record neuronal electrical activity in the SCN. The recording site is shown in close up on Right (a1), with dotted white lines delineating the SCN area and electrodes designated as within the SCN shown in blue. (B) Neuronal MUA recorded at the array of electrodes for the preparation shown in A as a function of projected ZT for a 24-h recording epoch. Spontaneous activity within the SCN (bounded by dotted lines) is higher than surrounding hypothalamus and plotted on a different scale (scale bars to right). (C) Time-averaged firing rate (MUA) across 24-h recording epochs from all channels covering SCN harvested from bright ($n = 92$ channels from four slices) versus dim ($n = 99$ channels from four slices) conditions. (D) Percentage of channels within the SCN classified as rhythmic for each experimental condition (bright versus dim, $**P < 0.01$; Fisher's exact test, data from four slices per condition). (E and F) Multitunit firing rate as a function of projected ZT for rhythmic recording sites within the SCN from animals maintained under bright (E) and dim (F) daytime conditions (bright, $n = 58$; dim, $n = 42$ channels; from a total of four animals per condition). (G) Peak-to-trough amplitude in the multitunit firing rhythm was significantly lower under dimmer lights. ($***P < 0.001$, Mann-Whitney U test, bright, $n = 58$; dim, $n = 42$ channels). Gray background indicates the projected period of lights off (ZT12 to ZT24). Data are expressed as mean \pm SEM.

ensemble has peak activity at that phase (37)] and results in substantially blunted circadian amplitude. Thus, both MEA and whole-cell recordings reveal that circadian differences in SFR and RMP at the population level are significantly smaller in the dim condition.

As experimental alterations in SCN electrical activity can influence the amplitude of circadian rhythms (43, 44), a parsimonious explanation for our findings is that the reduction in daytime depolarization is a primary impact of changing LD cycle amplitude, with knock-on impacts on the amplitude of SCN firing-rate rhythms and the robustness of rhythms at the whole-animal level. Future work will be required to determine how the difference in daytime RMP arises. Our whole-cell recordings preclude overall changes in input resistance or the frequency/amplitude of synaptic input as origins for this effect. This suggests a change in the magnitude of some other subtle depolarizing inward cation currents, acting as a driving force to promote excitability (45). Indeed, the high input resistance of SCN neurons (31) (including those of *R. pumilio*) means that even small differences in a depolarizing current could result in physiologically relevant changes in RMP. Alterations in SCN transcriptome and/or posttranslational modifications (e.g., phosphorylation) of ion channels or associated auxiliary proteins induced by high daytime light intensity offers a plausible explanation for the observed changes in RMP (46). Future studies combining electrophysiological recordings with single-cell RNA-sequencing as well as phosphoproteomic analysis would provide a better insight into potential molecular mechanisms underlying intrinsic changes in SCN neurophysiology in response to bright daytime light.

Another possibility, and one which cannot be determined with our methodology, is that exposure to different light intensities may alter the polarity of GABAergic activity in the SCN. GABA is the main neurotransmitter in the SCN, and the balance between its excitatory and inhibitory effects is key in shaping excitability and neuronal network dynamics in this brain region (47). Indeed, shifts in the inhibitory/excitatory ratio of GABAergic activity is well known to occur with environmental changes such as photoperiods, where increased light exposure favors the excitatory actions of GABA (48).

Importantly, the difference in daytime RMP and SFR is not simply an immediate response to exposure of light differing in intensity. The primary neurotransmitter of the retinohypothalamic tract is glutamate (49), but the SCN network principally employs GABA. Accordingly, in other species, individual SCN neurons can respond to light exposure either with inhibition or excitation (50). Although the literature is sparse, inhibitory responses may be more common in diurnal than nocturnal species (51, 52). Nevertheless, even if we accept that the immediate effect of light is mostly to excite the *R. pumilio* SCN, that cannot explain our observations, as both our MEA and whole-cell recordings are undertaken at least several hours after any direct drive from the retina has been removed (53). This implies that the effect of changing daytime irradiance on SCN neurophysiology is long lasting. That conclusion is supported by our finding that effects of the prior LD cycle on activity rhythms persist into subsequent free run in constant darkness. Previous research (54) has demonstrated that epigenetic modifications are at the core of the long-lasting effects on circadian period observed in young animals exposed to altered day length.

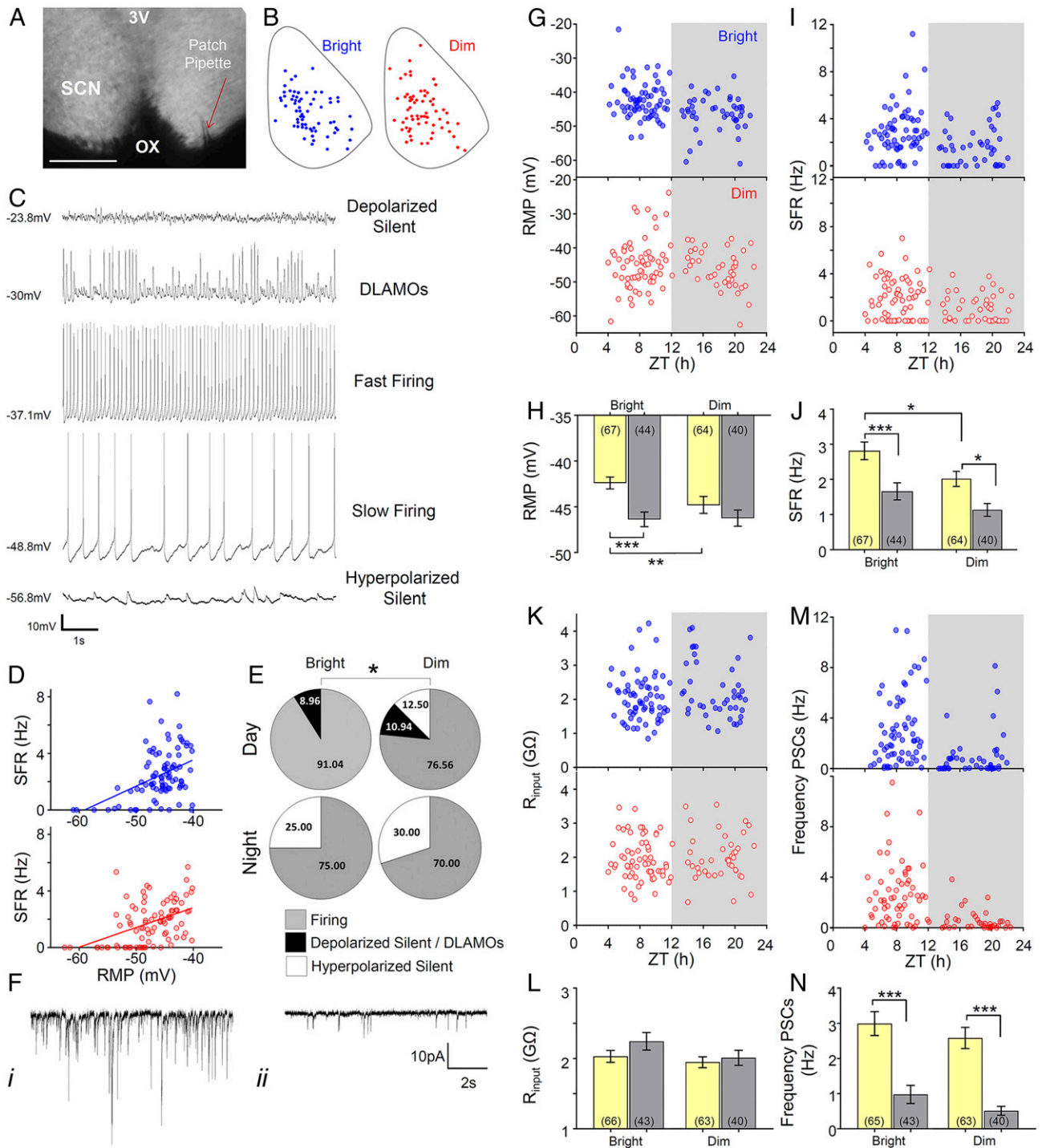


Fig. 4. Increasing daytime light intensity impacts SCN neurophysiology at the single-cell level. (A) Whole-cell recording setup showing bright-field image (4x) of a living SCN in coronal brain slice either side of the third ventricle (3V) and above the optic chiasm (OX), with a patch pipette (red arrow) targeting an SCN neuron. (Scale bar, 200 μ m.) (B) Schematic diagram showing the approximate location within a representative SCN coronal slice of the recorded cells giving rise to the daytime datasets under bright (blue) or dim (red) daytime irradiance. Note the similar spatial distribution between experimental groups. (C) Representative traces for each of the spontaneous membrane excitability states encountered in *R. pumilio* SCN neurons (from Top): highly depolarized silent; depolarized displaying low-amplitude membrane oscillations (DLAMOs); moderate RMP and firing at high or low rate; and hyperpolarized silent. (D) Positive correlation between RMP and SFR for cells recorded from bright (blue) and dim (red) conditions. Cells resting at RMP > -40 mV were excluded. $P < 0.0001$, linear regression analysis. (E) Pie charts showing the percentages of cells in the different electrophysiological states during the day and at night from bright and dim conditions. ($*P = 0.01$, chi-squared test.) (F) Example of traces from two SCN neurons (voltage clamped at -70 mV) showing PSCs recorded during the day (i) and at night (ii). (i) Cell displaying high frequency and amplitude PSCs; (ii) cell showing low frequency and amplitude PSCs. (G) Scatter plot showing the RMP of the different cells across ZTs for bright (blue) and dim (red) conditions. Each dot represents an individual cell. Gray background indicates the projected phase of lights off. (H) Mean RMP during the day and at night for SCN neurons from bright or dim conditions. (I and J) Same as in G and H but for SFR. (K and L) Same as in G and H but for Rinput. (M and N) Same as in G and H but for synaptic activity frequency. Data in bar charts are expressed as mean \pm SEM. Number of cells used is indicated between brackets in each bar. $*P < 0.05$, $**P \leq 0.01$, and $***P \leq 0.001$, Mann-Whitney *U* test.

Future work will be required to investigate if epigenetic changes contribute to the long-term effects observed in our study.

The question of how brighter daytime light impacts the circadian clock is of more than academic interest. The potential for light exposure at night to disrupt circadian clocks (with potentially wide-ranging impacts on physiology and well-being) is well established (55). The demonstration here that lower daytime irradiance can result in reduced circadian amplitude provides motivation to consider also the importance of daytime light exposure and a potential explanation for the beneficial effects of daytime light on circadian rhythms and sleep (10–18, 24, 25, 56, 57). The light intensities employed here span a range of plausible indoor light intensities. The lowest (corresponding to around 20 lx photopic illuminance of natural daylight [Melanopic EDI] or 40 lx photopic illuminance for a typical 3,000 K fluorescent source) would be that of a dimly lit room, while the brightest (equivalent of around 1,800 lx Melanopic EDI) would be of a bright room, likely with substantial natural light. Humans increasingly spend much of their day indoors exposed to light intensities far below those typical of outdoor daylight. This is particularly the case for some of the most vulnerable population groups, including hospital inpatients and care-home residents [who may have a predisposition for low circadian amplitude (58–60)]. Our findings suggest that, by reducing circadian amplitude, dim daytime light could contribute to some of the disruptions in sleep and circadian organization that such people suffer. As there is evidence that low amplitude also makes circadian clocks more susceptible to the disruptive effects of nocturnal light, it could also contribute to the widespread occurrence of social jetlag and chronic sleep deprivation in the general population. A standing question is whether any of the beneficial effects of brighter daytime light seen here can be recreated with shorter exposures to high irradiance. Nevertheless, our data provide a mechanistic justification for spending time outdoors during the day or enhancing indoor lighting for therapeutic purposes.

Materials and Methods

Animals. All animal use was in accordance with the UK Animals, Scientific Procedures Act of 1986 and was approved by the University of Manchester Ethics committee.

A total of 36 *R. pumilio* adults (male and female, age 3 to 9 mo) were used. Unless otherwise stated, animals were individually housed under a 12:12-h LD cycle and 22 °C ambient temperature in light tight cabinets. Zeitgeber time (ZT) 0 corresponds to the time of lights on, and ZT12 to lights off. Food and water were available ad libitum. Cages were equipped with running wheels (8.8 cm radius) for environmental enrichment.

Lighting Conditions. Light was measured using a calibrated spectroradiometer (SpectroCAL MSII, Cambridge Research Systems) at the cage level between 380 to 700 nm. Light was provided by smart red, green, blue, and white (RGBW) bulbs (LIFX A60; LIFX) in which light-emitting diode (LED) intensities could be independently controlled. Light stimuli aimed to approximate the relative activation for melanopsin, rods, and cones photoreceptors produced by natural daylight in the *R. pumilio*. Light intensity was reduced over two decades (bright, mid, dim, and dimmest) by introducing neutral density filters (Lee Filters) instead of reducing bulbs outputs in order avoid changes in ambient temperature. The effective photon flux for each photoreceptor (Fig. 1A) was calculated by multiplying the spectral power distribution of each light stimulus by the spectral sensitivity of each photopigment corrected for the *R. pumilio* spectral lens transmission (61). Corresponding Melanopic EDI lux were calculated using the CIE S 026 Toolbox (62).

Experimental Design for Behavioral Studies. Animals were housed under a stable 12:12 LD cycle with daytime light intensities ranging from bright, 14.80; mid, 13.66; dim, 12.95; to dimmest, 12.77 log effective photon flux/cm²/s for melanopsin. Each irradiance ran for 2 wk and ended with 4 d under constant darkness. We studied a total of 12 animals split over three different batches in which different daytime irradiances were presented in a pseudorandom order. (Batch 1 (*n* = 5): mid, dim, bright, dimmest; Batch 2 (*n* = 2): dimmest, mid, bright, dim; and Batch 3 (*n* = 5): bright, dim, mid, dimmest.)

Activity and Tb rhythms were recorded throughout the whole experiment. Home cage activity was monitored in 10-s bins using a passive infrared motion

sensor system, as previously described (63, 64). Wheel-running activity was continuously recorded as wheel revolutions/10-s intervals using a custom-made data acquisition system. Tb was recorded every 30 min using a data logger (Maxim, DS1922L-F5; ThermoChron; Data loggers iButton; Maxim Integrated Products). iButtons were dehusked and potted with wax (20% Poly(ethylene-covinyl acetate) and 80% paraffin mixture) before surgical implantation into the peritoneal cavity (65).

Brain-Slice Preparation for Electrophysiological Recordings. *R. pumilio*, housed either under bright (*n* = 12) or dim (*n* = 12) daytime conditions for 2 to 3 wk, were sedated with isoflurane (Abbott Laboratories) and immediately culled by cervical dislocation during the light phase (beginning of the day or late day). Brain slices were prepared as described previously (66). Briefly, following euthanasia, brains were removed and mounted onto a metal stage. Coronal slices containing mid-SCN levels across the rostro-caudal axis were cut using a Campden 7000smz-2 vibrating microtome (Campden Instruments). Slices were cut at 250- μ m thickness for whole-cell recordings and at 350 μ m for long-term in vitro extracellular multielectrode recording. Slicing was done in an ice-cold (4 °C) sucrose-based incubation solution containing the following (in mM): 3 KCl, 1.25 NaH₂PO₄, 0.1 CaCl₂, 5 MgSO₄, 26 NaHCO₃, 10 D-glucose, 189 sucrose, oxygenated with 95% O₂, 5% CO₂. After cutting, slices were left to recover at room temperature in a holding chamber with continuously gassed incubation solution for at least 20 min before transferring into artificial cerebrospinal fluid (aCSF). Recording aCSF has the following composition (in mM): 124 NaCl, 3 KCl, 24 NaHCO₃, 1.25 NaH₂PO₄, 1 MgSO₄, 10 D-Glucose, 2 CaCl₂, and 0 sucrose. For long-term in vitro recordings, aCSF was supplemented with 0.001% gentamicin (Sigma-Aldrich). Slices were allowed to rest for at least 20 min before placement in the recording chamber of the MEA or the upright microscope where they were continuously perfused with continuously gassed aCSF for the entire recording (~3 mL/min in the MEA and ~2.5 mL/min in the microscope).

In Vitro Extracellular Multielectrode Recordings. Recordings were performed from slices prepared in the late afternoon using 60pMEA100/30IR-Ti-gr perforated MEAs comprising 59 electrodes (100 μ m apart and arranged in a 6 × 10 layout, see Fig. 3A) as previously described (66). Optimal brain-slice positioning and aligning onto the recording electrodes were confirmed by overlaying images captured with a GXCAM-1.3 camera (GX Optical) fitted to a dissecting microscope. MEA recordings were performed at 34 °C.

Data were sampled at 50 kHz with MC_Rack Software using a USB-ME64 system and MEA 1060UP-BC amplifier from Multi-Channel Systems (GmbH). Data were then high-pass filtered at 200 Hz and second order Butterworth. Events/spikes were extracted by setting up a threshold (−17.5 μ V) based on baseline noise level measured during tetrodotoxin (TTX) treatment. Baseline MUA levels were recorded for a period >24 h. At the end of each experiment, the glutamate agonist NMDA (20 μ M) was bath applied for 5 min to confirm maintained cell responsiveness, followed by 1 μ M TTX (~8 min) to confirm acquired signals exclusively reflected Na⁺-dependent action potentials. All drugs were purchased from Tocris Bioscience and stored as stock solutions (prepared in purified dH₂O) at −20 °C. Drugs were diluted to their respective final concentrations directly in prewarmed, oxygenated aCSF on the experimental day.

Whole-Cell Voltage- and Current-Clamp Recordings. Coronal brain slices containing midlevel of the SCN (250 μ m) were placed in the bath chamber of an upright Leica epi-fluorescence microscope (DMLFS; Leica Microsystems Ltd) equipped with infrared video-enhanced differential interference contrast optics. Slices were held in place with a tissue anchor grid and continuously perfused with aCSF by gravity. Recordings were performed from neurons located across the whole SCN (Fig. 4A) during the day and at night. SCN neurons were identified with a 40 \times water immersion UV objective (HCX APO; Leica) and targeted using a cooled Teledyne Photometrics camera (Retiga Electro). Photographs of the patch pipette sealed to SCN neurons were taken at the end of each recording for accurate confirmation of anatomical location of the recorded cell within the SCN.

Patch pipettes (resistance 7 to 10 M Ω) were fashioned from thick-walled borosilicate glass capillaries (Harvard Apparatus) pulled using a two-stage micropipette puller (PB-10; Narishige). Recording pipettes were filled with an intracellular solution containing the following (in mM): 120 K-gluconate, 20 KCl, 2 MgCl₂, 2 K₂-ATP, 0.5 Na-GTP, 10 Hepes, and 0.5 EGTA, pH adjusted to 7.3 with KOH, measured osmolality 295 to 300 mOsmol/kg. Cell membrane was ruptured at −70 mV under minimal holding negative pressure.

An Axopatch Multiclamp 700A amplifier (Molecular Devices) was used in voltage-clamp and current-clamp modes. Signals were sampled at 25 kHz and acquired in gap-free mode using pClamp 10.7 (Molecular Devices).

Access resistance for the cells used for analysis was $<30\text{ M}\Omega$, and series resistance was below $50\text{ M}\Omega$. PSCs were measured under voltage-clamp mode while holding the cells at -70 mV . Measurement of spontaneous activity in current-clamp mode was performed with no holding current ($I = 0$). All data acquisition and protocols were generated through a Digidata 1322A interface (Molecular Devices). All recordings were performed at room temperature ($\sim 23\text{ }^\circ\text{C}$). A portion of the data appearing in this study also contributed to the detailed analysis of the electrophysiological properties of *R. pumilio* SCN in Bano-Otalora et al. (67)

Data and Statistical Analysis.

Analysis of behavioral and physiological data. General activity, voluntary wheel-running activity, and Tb actograms were generated using El Temps (El Temps version 1.228; © Díez Noguera, University of Barcelona). Averaged mean waveforms and quantitative analysis of activity, sustained immobility, and Tb patterns under LD conditions were calculated based on data (in 30-min bins) across the last 8 d of each lighting stage. Intradaily variability, a measure of rhythm fragmentation within a day, and day-to-day stability (interdaily stability) for each rhythm were calculated as previously described (68). Sustained immobility (which in mice corresponds to episodes of sleep) was defined as a period of immobility $>40\text{ s}$, based on published criteria (63).

To calculate the phase angle of entrainment and circadian period of the activity rhythm, three experienced scorers, blind to the lighting conditions, fitted a line across activity onsets under constant dark conditions. Phase angle of entrainment was expressed as the predicted time of activity onset on the last day under LD conditions by extrapolation of the fitted line. Values reported in the manuscript are the average of those obtained by the three investigators. %V in activity accounted for by the circadian period was determined by Sokolove-Bushell periodogram (El Temps version 1.228) and used as an indicator of rhythm robustness under constant darkness. Relationship between daytime irradiance and different rhythm parameters was evaluated by linear regression analysis, with $P < 0.05$ indicating that the slope of the fitted line is significantly nonzero.

Analysis of extracellular multielectrode recordings. Long-term MEA recordings were analyzed using custom Matlab routines as previously described (66). MUA recorded by each electrode/channel was considered to exhibit circadian variation when better fit by a sinusoidal function (constrained to a

periodicity between 20 and 28 h) than a first-order polynomial. Peak and trough firing for each rhythmic channel was determined from a 60 s binned time-series (smoothed with a 2-h boxcar filter). Percentages of rhythmic versus nonrhythmic channels between lighting conditions were compared using Fisher's exact test.

Analysis of whole-cell recordings. PSCs frequency and amplitude (threshold of 5 pA) analysis was performed offline by template-based sorting in Clampfit 10.7 (Molecular Devices) within a 30-s window as previously described (69). Current-clamp data were analyzed using Spike2 software (Cambridge Electronic Design). RMP, SFR, and input resistance (R_{input}) were determined within 5 min of membrane rupture. Average SFR in firing cells was calculated as the number of action potentials per second within a 30-s window of stable firing using a custom-written Spike2 script, and average RMP was measured as the mean voltage over a 30-s window. R_{input} was estimated using Ohm's law ($R = V/I$) where V represents the change in voltage induced by a hyperpolarizing current pulse (-30 pA for 500 ms) as previously described (31). Percentages of cells in the different electrophysiological states during the day and at night from bright and dim conditions were analyzed using chi-squared test.

Statistical analysis. Nonnormal distributed electrophysiological data from different lighting conditions and time of day were compared using Mann-Whitney U test. All statistical analysis were performed using SPSS version 23 (SPSS Inc.) and GraphPad Prism 7.04 (GraphPad Software Inc.). For all tests, statistical significance was set at $P < 0.05$. Data are expressed as mean \pm SEM. Sample sizes are indicated throughout the text and figure legends.

Data Availability. All study data are included in the article and/or *SI Appendix*.

ACKNOWLEDGMENTS. We thank the members of the University of Manchester Biological Services Facility and Jonathan Wynne for their excellent assistance in colony maintenance and husbandry. We also thank Professor Simon Luckman for allowing us access to his electrophysiology equipment and Dr. Josh Moulard for his assistance with light measurements. This work was funded by a Biotechnology and Biological Sciences Research Council (BBSRC) Industrial Partnership Award with Signify (BB/P009182/1) to R.J.L. and T.M.B., by grants from the BBSRC to T.M.B. (B/N014901/1) and to M.D.C.B. (BB/S01764X/1), and the Wellcome Trust (210684/Z/18/Z) to R.J.L.

1. B. Bano-Otalora, H. D. Piggins, "The mammalian neural circadian system: From molecules to behaviour" in *Biological Timekeeping: Clocks, Rhythms and Behaviour*, V. Kumar, Ed. (Springer India, New Delhi, 2017), pp. 257–275.
2. J. A. Mohawk, C. B. Green, J. S. Takahashi, Central and peripheral circadian clocks in mammals. *Annu. Rev. Neurosci.* **35**, 445–462 (2012).
3. M. D. C. Belle, C. O. Diekmann, Neuronal oscillations on an ultra-slow timescale: Daily rhythms in electrical activity and gene expression in the mammalian master circadian clockwork. *Eur. J. Neurosci.* **48**, 2696–2717 (2018).
4. T. M. Brown, H. D. Piggins, Electrophysiology of the suprachiasmatic circadian clock. *Prog. Neurobiol.* **82**, 229–255 (2007).
5. T. M. Brown, Using light to tell the time of day: Sensory coding in the mammalian circadian visual network. *J. Exp. Biol.* **219**, 1779–1792 (2016).
6. S. Daan, C. S. Pittendrigh, A functional analysis of circadian pacemakers in nocturnal rodents. *J. Comp. Physiol.* **106**, 253–266 (1976).
7. J. F. Duffy, C. A. Czeisler, Effect of light on human circadian physiology. *Sleep Med. Clin.* **4**, 165–177 (2009).
8. R. E. Kronauer, "A quantitative model for the effects of light on the amplitude and phase of the deep circadian pacemaker, based on human data" in *Proceedings of the Tenth European Congress on Sleep Research*, J. Horne, Ed. (Pontenagel Press, Dusseldorf, Germany, 1990), p. 306.
9. C. S. Pittendrigh, "Circadian systems: Entrainment" in *Handbook of Behavioral Neurobiology: Biological Rhythms*, J. Aschoff, Ed. (Plenum Press, New York, 1981), pp. 95–124.
10. K. P. Wright Jr et al., Entrainment of the human circadian clock to the natural light-dark cycle. *Curr. Biol.* **23**, 1554–1558 (2013).
11. K. V. Danilenko, I. L. Plisov, A. Wirz-Justice, M. Hebert, Human retinal light sensitivity and melatonin rhythms following four days in near darkness. *Chronobiol. Int.* **26**, 93–107 (2009).
12. K. Mishima, M. Okawa, T. Shimizu, Y. Hishikawa, Diminished melatonin secretion in the elderly caused by insufficient environmental illumination. *J. Clin. Endocrinol. Metab.* **86**, 129–134 (2001).
13. S. Ancoli-Israel et al., Increased light exposure consolidates sleep and strengthens circadian rhythms in severe Alzheimer's disease patients. *Behav. Sleep Med.* **1**, 22–36 (2003).
14. K. Mishima, Y. Hishikawa, M. Okawa, Randomized, dim light controlled, crossover test of morning bright light therapy for rest-activity rhythm disorders in patients with vascular dementia and dementia of Alzheimer's type. *Chronobiol. Int.* **15**, 647–654 (1998).
15. M. Münch et al., Bright light delights: Effects of daily light exposure on emotions, reactivity cycles, sleep and melatonin secretion in severely demented patients. *Curr. Alzheimer Res.* **14**, 1063–1075 (2017).
16. E. J. Van Someren, A. Kessler, M. Mirmiran, D. F. Swaab, Indirect bright light improves circadian rest-activity rhythm disturbances in demented patients. *Biol. Psychiatry* **41**, 955–963 (1997).
17. P. D. Sloane et al., High-intensity environmental light in dementia: Effect on sleep and activity. *J. Am. Geriatr. Soc.* **55**, 1524–1533 (2007).
18. G. J. Hjetland et al., Light interventions and sleep, circadian, behavioral, and psychological disturbances in dementia: A systematic review of methods and outcomes. *Sleep Med. Rev.* **52**, 101310 (2020).
19. W. Witting, M. Mirmiran, N. P. Bos, D. F. Swaab, Effect of light intensity on diurnal sleep-wake distribution in young and old rats. *Brain Res. Bull.* **30**, 157–162 (1993).
20. S. E. Labyak, F. W. Turek, E. P. Wallen, P. C. Zee, Effects of bright light on age-related changes in the locomotor activity of Syrian hamsters. *Am. J. Physiol.* **274**, R830–R839 (1998).
21. J. L. Soman, A. M. Tinga, S. F. Te Pas, R. van Ee, B. N. S. Vlaskamp, Acute alerting effects of light: A systematic literature review. *Behav. Brain Res.* **337**, 228–239 (2018).
22. P. Badia, B. Myers, M. Boecker, J. Culpepper, J. R. Harsh, Bright light effects on body temperature, alertness, EEG and behavior. *Physiol. Behav.* **50**, 583–588 (1991).
23. C. Cajochen, Alerting effects of light. *Sleep Med. Rev.* **11**, 453–464 (2007).
24. R. T. Dauchy et al., Effects of daytime exposure to light from blue-enriched light-emitting diodes on the nighttime melatonin amplitude and circadian regulation of rodent metabolism and physiology. *Comp. Med.* **66**, 373–383 (2016).
25. N. N. Takasu et al., Repeated exposures to daytime bright light increase nocturnal melatonin rise and maintain circadian phase in young subjects under fixed sleep schedule. *Am. J. Physiol. Regul. Integr. Comp. Physiol.* **291**, R1799–R1807 (2006).
26. S. Hashimoto et al., Midday exposure to bright light changes the circadian organization of plasma melatonin rhythm in humans. *Neurosci. Lett.* **221**, 89–92 (1997).
27. D. A. Dewsbury, W. W. Dawson, African four-striped grass mice (*Rhabdomys pumilio*), a diurnal-crepuscular murid rodent, in the behavioral laboratory. *Behav. Res. Meth. Instrum.* **11**, 329–333 (1979).
28. D. M. Schumann, H. M. Cooper, M. D. Hofmeyr, N. C. Bennett, Circadian rhythm of locomotor activity in the four-striped field mouse, *Rhabdomys pumilio*: A diurnal African rodent. *Physiol. Behav.* **85**, 231–239 (2005).
29. I. van der Merwe, M. K. Oosthuizen, A. Ganswindt, A. Haim, N. C. Bennett, Effects of photophase illumination on locomotor activity, urine production and urinary 6-sulfatoxymelatonin in nocturnal and diurnal South African rodents. *J. Exp. Biol.* **220**, 1684–1692 (2017).
30. S. P. Fisher et al., Rapid assessment of sleep-wake behavior in mice. *J. Biol. Rhythms* **27**, 48–58 (2012).
31. M. D. Belle, C. O. Diekmann, D. B. Forger, H. D. Piggins, Daily electrical silencing in the mammalian circadian clock. *Science* **326**, 281–284 (2009).

32. C. O. Diekmann *et al.*, Causes and consequences of hyperexcitation in central clock neurons. *PLoS Comput. Biol.* **9**, e1003196 (2013).
33. M. U. Gillette *et al.*, Intrinsic neuronal rhythms in the suprachiasmatic nuclei and their adjustment. *Ciba Found. Symp.* **183**, 134–144, discussion 144–153 (1995).
34. J. H. Meijer, J. Schaap, K. Watanabe, H. Albus, Multiunit activity recordings in the suprachiasmatic nuclei: In vivo versus in vitro models. *Brain Res.* **753**, 322–327 (1997).
35. T. Sato, H. Kawamura, Circadian rhythms in multiple unit activity inside and outside the suprachiasmatic nucleus in the diurnal chipmunk (*Eutamias sibiricus*). *Neurosci. Res.* **1**, 45–52 (1984).
36. N. F. Ruby, H. C. Heller, Temperature sensitivity of the suprachiasmatic nucleus of ground squirrels and rats in vitro. *J. Biol. Rhythms* **11**, 126–136 (1996).
37. S. Paul *et al.*, Output from VIP cells of the mammalian central clock regulates daily physiological rhythms. *Nat. Commun.* **11**, 1453 (2020).
38. M. E. Jewett, R. E. Kronauer, C. A. Czeisler, Light-induced suppression of endogenous circadian amplitude in humans. *Nature* **350**, 59–62 (1991).
39. A. C. West *et al.*, Misalignment with the external light environment drives metabolic and cardiac dysfunction. *Nat. Commun.* **8**, 417 (2017).
40. H. T. VanderLeest *et al.*, Seasonal encoding by the circadian pacemaker of the SCN. *Curr. Biol.* **17**, 468–473 (2007).
41. J. Rohling, J. H. Meijer, H. T. VanderLeest, J. Admiraal, Phase differences between SCN neurons and their role in photoperiodic encoding; a simulation of ensemble patterns using recorded single unit electrical activity patterns. *J. Physiol. Paris* **100**, 261–270 (2006).
42. M. R. Ruijck *et al.*, Evidence for weakened intercellular coupling in the mammalian circadian clock under long photoperiod. *PLoS One* **11**, e0168954 (2016).
43. J. P. Whitt, J. R. Montgomery, A. L. Meredith, BK channel inactivation gates daytime excitability in the circadian clock. *Nat. Commun.* **7**, 10837 (2016).
44. T. Kudo, D. H. Loh, D. Kuljis, C. Constance, C. S. Colwell, Fast delayed rectifier potassium current: Critical for input and output of the circadian system. *J. Neurosci.* **31**, 2746–2755 (2011).
45. M. Flourakis *et al.*, A conserved bicycle model for circadian clock control of membrane excitability. *Cell* **162**, 836–848 (2015).
46. C. S. Colwell, Linking neural activity and molecular oscillations in the SCN. *Nat. Rev. Neurosci.* **12**, 553–569 (2011).
47. H. E. Albers, J. C. Walton, K. L. Gamble, J. K. McNeill IV, D. L. Hummer, The dynamics of GABA signaling: Revelations from the circadian pacemaker in the suprachiasmatic nucleus. *Front. Neuroendocrinol.* **44**, 35–82 (2017).
48. S. Farajnia, T. L. van Westering, J. H. Meijer, S. Michel, Seasonal induction of GABAergic excitation in the central mammalian clock. *Proc. Natl. Acad. Sci. U.S.A.* **111**, 9627–9632 (2014).
49. L. P. Morin, C. N. Allen, The circadian visual system, 2005. *Brain Res. Brain Res. Rev.* **51**, 1–60 (2006).
50. T. M. Brown, J. Wynne, H. D. Piggins, R. J. Lucas, Multiple hypothalamic cell populations encoding distinct visual information. *J. Physiol.* **589**, 1173–1194 (2011).
51. Y. Y. Jiao, T. M. Lee, B. Rusak, Photic responses of suprachiasmatic area neurons in diurnal degus (*Octodon degus*) and nocturnal rats (*Rattus norvegicus*). *Brain Res.* **817**, 93–103 (1999).
52. J. H. Meijer, B. Rusak, M. E. Harrington, Photically responsive neurons in the hypothalamus of a diurnal ground squirrel. *Brain Res.* **501**, 315–323 (1989).
53. S. J. Kuhlman, R. Silver, J. Le Sauter, A. Bult-Itto, D. G. McMahon, Phase resetting light pulses induce Per1 and persistent spike activity in a subpopulation of biological clock neurons. *J. Neurosci.* **23**, 1441–1450 (2003).
54. A. Azzi *et al.*, Circadian behavior is light-reprogrammed by plastic DNA methylation. *Nat. Neurosci.* **17**, 377–382 (2014).
55. I. C. Mason *et al.*, Circadian health and light: A report on the national heart, lung, and blood institute's workshop. *J. Biol. Rhythms* **33**, 451–457 (2018).
56. E. J. Wams *et al.*, Linking light exposure and subsequent sleep: A field polysomnography study in humans. *Sleep (Basel)* **40**, zsx165 (2017).
57. M. Boubekri, I. N. Cheung, K. J. Reid, C. H. Wang, P. C. Zee, Impact of windows and daylight exposure on overall health and sleep quality of office workers: A case-control pilot study. *J. Clin. Sleep Med.* **10**, 603–611 (2014).
58. S. Hood, S. Amir, The aging clock: Circadian rhythms and later life. *J. Clin. Invest.* **127**, 437–446 (2017).
59. S. Farajnia *et al.*, Evidence for neuronal desynchrony in the aged suprachiasmatic nucleus clock. *J. Neurosci.* **32**, 5891–5899 (2012).
60. T. J. Nakamura *et al.*, Age-related decline in circadian output. *J. Neurosci.* **31**, 10201–10205 (2011).
61. A. E. Allen *et al.*, Spectral sensitivity of cone vision in the diurnal murid *Rhabdomys pumilio*. *J. Exp. Biol.* **223**, jeb215368 (2020).
62. International Commission on Illumination, "CIE system for metrology of optical radiation for iPRGC-influenced responses to light" in *Report CIE S 026/E:2018* (CIE, Vienna, Austria, 2018), p. 32.
63. L. A. Brown, S. Hasan, R. G. Foster, S. N. Peirson, COMPASS: Continuous open mouse phenotyping of activity and sleep status. *Wellcome Open Res.* **1**, 2 (2016).
64. J. W. Moulard, F. Martial, A. Watson, R. J. Lucas, T. M. Brown, Cones support alignment to an inconsistent world by suppressing mouse circadian responses to the blue colors associated with twilight. *Curr. Biol.* **29**, 4260–4267.e4 (2019).
65. B. G. Lovegrove, Modification and miniaturization of ThermoChron iButtons for surgical implantation into small animals. *J. Comp. Physiol. B* **179**, 451–458 (2009).
66. L. Hanna, L. Walmsley, A. Pienaar, M. Howarth, T. M. Brown, Geniculohypothalamic GABAergic projections gate suprachiasmatic nucleus responses to retinal input. *J. Physiol.* **595**, 3621–3649 (2017).
67. B. Bano-Otalora *et al.*, Daily electrical activity in the master circadian clock of a diurnal mammal <https://doi.org/10.1101/2020.12.23.424225> (23 December 2020).
68. E. J. van Someren *et al.*, Circadian rest-activity rhythm disturbances in Alzheimer's disease. *Biol. Psychiatry* **40**, 259–270 (1996).
69. M. D. Belle, H. D. Piggins, Circadian regulation of mouse suprachiasmatic nuclei neuronal states shapes responses to orexin. *Eur. J. Neurosci.* **45**, 723–732 (2017).